UWB Connectivity Inside a Space Launch Vehicle

Daniel Neuhold[1], Jorge F. Schmidt[1,2], Christian Bettstetter[1,2], Johannes Sebald[3], and Jirka Klaue[4]
[1]University of Klagenfurt, Institute of Networked and Embedded Systems, Austria
[2]Lakeside Labs GmbH, Klagenfurt, Austria
[3]ArianeGroup, Bremen, Germany
[4]Airbus, Hamburg, Germany

***Abstract*—Measurements of ultra-wideband (UWB) communications inside an Ariane 5 launcher are reported, assessing received signal power fluctuations and connectivity in the vehicle equipment bay. This environment is challenging due to shadowing and reflections. Our results highlight the relationship between the multipath delay spread and the UWB signal detection mechanism and indicate that UWB is a suitable candidate for radio connectivity inside launch vehicles.**

I. Introduction

Replacing the cables in a space launch vehicle by wireless connectivity can bring various benefits. For example, the mechanical stress on cables during liftoff would be avoided, the vehicle's mass be reduced, and the assembly would become more flexible. However, the deployment of an in-vehicle wireless system prompts various challenges and requires solutions that extend conventional short-range radio technologies available on the market. A particular challenge addressed in this paper is the connectivity inside the vehicle equipment bay (VEB). This ring-shaped unit, illustrated in Figure 1, surrounds the vehicle tank and contains most of the essential steering and controlling equipment. The unit is shielded and electronically decoupled from the rest of the launcher. It represents a Faraday cage with many reflections caused by integrated equipment and metal objects.

A promising radio technology for such extreme environments is *ultra-wideband* (UWB) communications. Its high data rate, precision in localization, robustness against narrowband interference, and low power consumption are unique features making it a candidate for applications in the VEB. In order to assess its feasibility, we deploy a sensor network inside the VEB of an Ariane 5 launcher. Off-the-shelf IEEE 802.15.4-2011 compliant transceivers from DecaWave are used and operated at a center frequency of 4.3 GHz with a bandwidth of 500 MHz. The received signal powers are analyzed for sensor nodes and access points placed at specific locations.

This work complements our previous results on UWB for airplanes [1] and infrared communications for launchers [2], [3], [4]. We present, for the first time, a proof-of-concept testbed for high-speed UWB communications in a launch vehicle and experimentally characterize the received signal powers.

Section II describes the experimental setup. Section III presents and discusses the results from our measurement campaign. Section IV covers related work. Section V concludes.

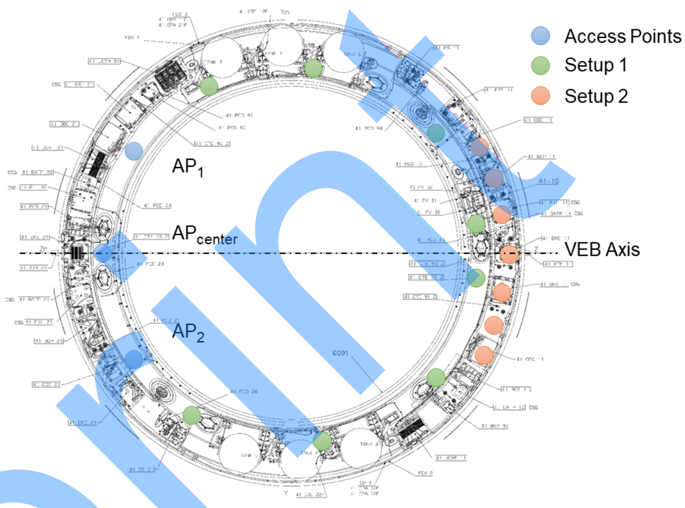

Fig. 1: Measurement setup in an Ariane 5 VEB. Outer diameter is 5.4 m. Diagram labels are unreadable on purpose.

II. Experimental Setup

A small UWB sensor network is deployed inside a full-sized Ariane 5 VEB. The VEB is electronically decoupled from the rest of the vehicle (the conductive cover plates on top of the VEB are fully attached), thus giving us real operational conditions. Figure 1 illustrates the VEB structure with its equipment. This environment poses two major design challenges: first, shadowing caused by the equipment is severe due to the large number and size of components (e.g., the spherical fuel tanks); and second, significant multipath propagation occurs as most of the equipment is covered with metal housings.

Up to eight UWB nodes are deployed at positions that correspond to sensor locations in the launcher. These nodes communicate with an access point (AP). We evaluate the received signal strength indicator (RSSI) and packet losses in the uplink from the nodes to the AP. The resulting radio connectivity sheds light on the capabilities of UWB in a launcher and ultimately on the number of APs needed to attain coverage of the VEB. All nodes operate with a data rate of 6.8 Mbps and a packet length of 1023 bytes. All devices are deployed at the same height and use the same hardware platform with their role defined by software.

Two setups are addressed. In the first setup, eight nodes (green dots in Fig. 1) are equally spaced along the VEB ring to communicate to a single AP. This AP is first positioned at AP_{center} and then relocated to AP_1 and AP_2 (blue dots). A time division multiple access (TDMA) scheme is used with a TDMA frame of one second. In a second setup, we explore in further detail the radio coverage of the area opposite to AP_{center}. We measure point-to-point links from seven critical node locations (orange dots) to the AP_{center}. Each link is evaluated individually for ten minutes.

III. Experimental Results

A. The RSSI values vary strongly over time.

The upper part of Figure 2 shows, for the first setup, the RSSI values (colored lines) and packet losses (crosses) over half an hour. Only three packets are lost. Our major observation from these measurements is that there are strong RSSI fluctuations. Such severe dynamics with power dips beyond 10 dB surprise us since it appears to be in contradiction to our previous measurements conducted with the same transceivers in a similar environment, namely in the cabin of an aircraft, where RSSI values are stable (see lower part of the figure).

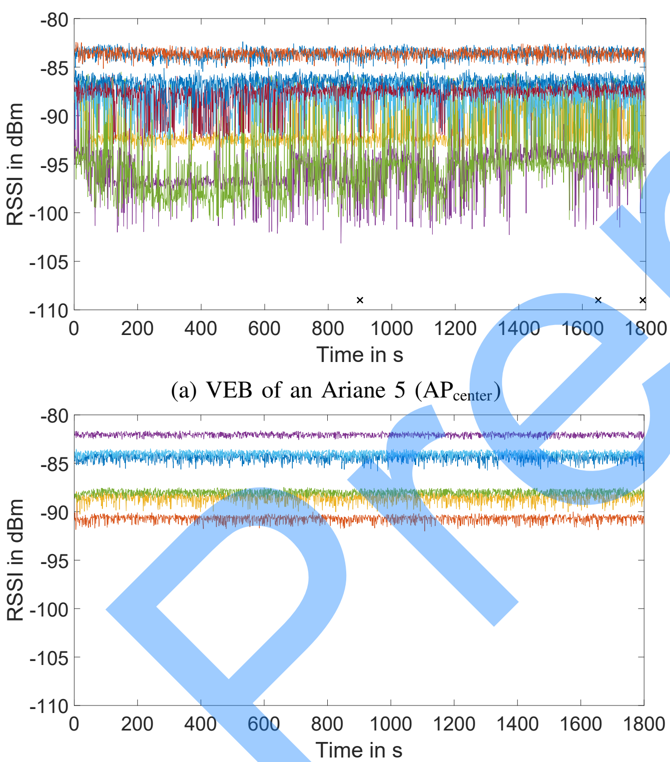

(a) VEB of an Ariane 5 (AP_{center})

(b) Passenger cabin of an Airbus A319 airplane

Fig. 2: Reception powers (lines) and packet losses (crosses).

Let us take a step back to find a potential cause for this phenomenon. In principle, power fluctuations over a radio channel arise from noise and fading due to the mobility of transceivers or obstacles. However, these cannot be the reasons for the fluctuations since our system is operated in a high-signal-to-noise-ratio regime and a static environment. Beyond this, the possibility of interference as a cause for

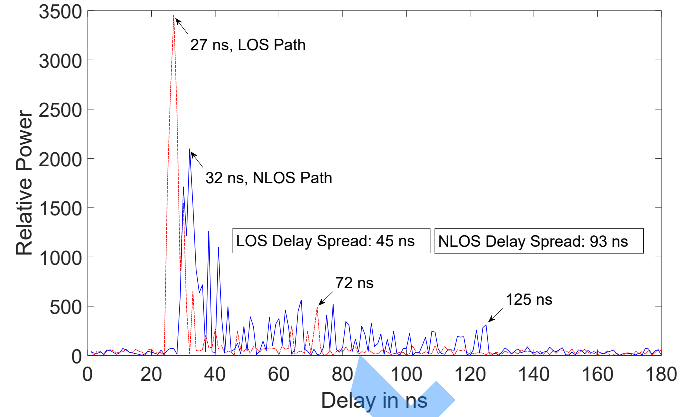

Fig. 3: Power delay profile for LOS and NLOS settings.

fluctuations is essentially ruled out by the electromagnetic isolation of the VEB. There remains another potential cause: fluctuations can be induced by particularities of the propagation environment that significantly deviate from those upon which the transceiver has been designed. Specifically, the signal power measurement procedure is linked to the number and separation of received multipath components. Here is a key difference between the VEB and an aircraft. In the VEB, the metallic ring-shaped environment favors many more multipath components reaching the receiver with comparable power levels. This is in contrast with the aircraft scenario with longer links and more energy absorption by the interior fittings.

To understand this behavior in more depth, we study the delay spread of the received signal in a controlled laboratory setup and relate it to the way in which RSSI values are computed by our transceiver. Two static setups are addressed: one with a line-of-sight (LOS) link between the transmitter and receiver, and another with non-line-of-sight (NLOS) conditions, in which an obstacle blocks the LOS path.

The relative power delay profiles (PDP) are shown in Figure 3. The NLOS setup has a stronger delay spread (93 ns) than the LOS setup (45 ns), mainly because the NLOS setup has more multipath components.

In order to relate the measured spreading to RSSI fluctuations, we need to know the internal computations of the transceiver. The handbook [5] states that two types of RSSI are calculated:

$$\mathrm{RSSI}_{\mathrm{FP}} = 10\log\left(\frac{F_1^2 + F_2^2 + F_3^2}{N^2}\right) - A \quad \text{and} \tag{1}$$

$$\mathrm{RSSI}_{\mathrm{PDP}} = 10\log\left(\frac{2^{17}C}{N^2}\right) - A\,. \tag{2}$$

The first expression estimates the received power in dBm using solely the first three peaks (amplitudes F_i with $i = 1, 2, 3$). They are normalized to the preamble accumulator count value N. The constant A in dBm depends on the pulse repetition frequency configuration of the transceiver. The second expression indicates the received power in dBm using the

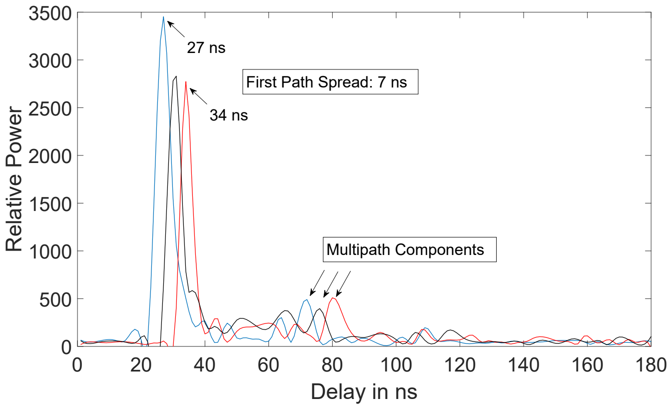

Fig. 4: Temporal fluctuation of PDP acquisition over successive packets in a static laboratory environment.

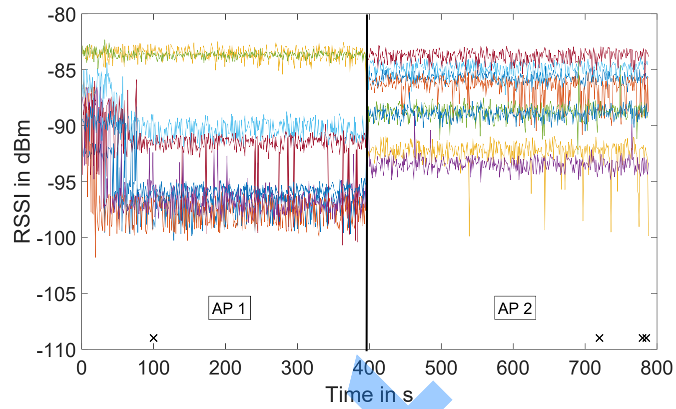

Fig. 5: Reception powers (lines) and packet losses (crosses).

accumulated squared channel impulse response magnitude C for the estimated highest power portion of the channel.

Expressions (1) and (2) are based on the received PDP. This entails that different peak amplitudes and spreading directly affect the RSSI estimates. However, the acquisition process of the PDP includes inaccuracies caused by accumulating and windowing energy detectors for the different channel taps at the receiver's analog front end. For very reflexive propagation environments, the signal power distributes over a large number of energy detectors, leading to low accuracy due to accumulation and windowing operations. The add-up of these tolerances yields slightly different PDPs over time, even when operating in a static environment. This effect is demonstrated in Figure 4, which shows three successive measurements of the PDP. Although the same qualitative PDP is observed, successive measurements yield different leading edge delays, peak powers, and oscillations.

These fluctuations in the PDP acquisition in combination with the above expressions can explain the RSSI fluctuations in our experiments. They also highlight the sensitivity of the PDP acquisition methodology with respect to the propagation environment. This in turn sets a limit — in terms of delay spread — on the scenarios in which UWB using this signal acquisition methodology can be accurately operated without further compensations.

B. The RSSI values are well above the receiver sensitivity.

We now study the radio coverage of different AP positions in the first setup. The RSSI and loss of packets from the different nodes to AP_1 and AP_2 are shown in Figure 5. Although the received power in AP_1 is on average lower and more dynamic than that in AP_2, both locations yield a suitable connectivity with a margin of more than 10 dB to the receiver sensitivity at -110 dBm.

C. One access point is sufficient for full coverage.

Some important node positions in the VEB suffer from higher attenuation and more frequent packet losses than other positions, due to longer distances and the location of equipment. These critical positions (orange dots in Fig. 1) are evaluated in our second setup for transmissions to the AP_{center}. Each link is evaluated independently from other links to enable intensive testing using more frequent packets.

The results in Figure 6 show sufficiently high reception powers for all positions, indicating that full coverage can be achieved for all evaluated positions with a single AP. The most severe dip goes down to -97 dBm. Transmissions from the node with the most distant position yield a stable reception power with small fluctuation. We conjecture that this behavior is a result of the accumulation of multipath components. It is observed for several positions, that have a higher and less fluctuating signal power despite a larger distance and more obstacles between the node and AP.

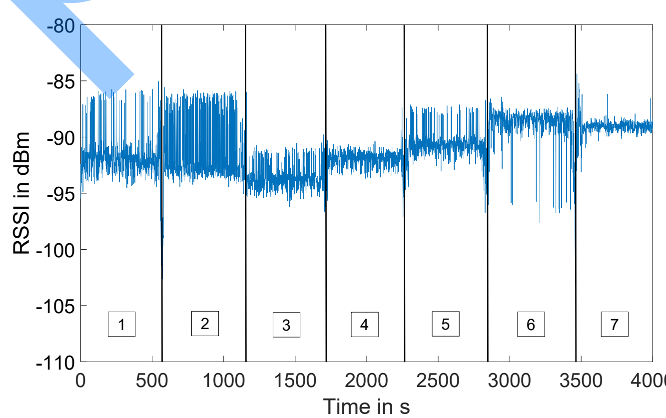

Fig. 6: Point-to-point connectivity of nodes (in setup 2 from bottom to top) to AP_{center}.

IV. Related Work

Most experimental work on UWB is on localization and tracking rather than communications. The field of UWB communications for space applications is only marginally explored. Similar work can be found on two topics: (1) UWB in airplanes and (2) other wireless technologies in launchers.

Airplanes have similar requirements and restrictions as launchers. The use of UWB for in-airplane systems is addressed in [6], [7], [8], [9], and [10], to give some examples. As opposed to expensive channel sounding [10], our work employs off-the-shelf transceivers. Condition monitoring for mechanical parts of an airplane is investigated in [11] and [12].

As an alternative wireless technology, infrared communications is considered to be safe for the integrated aviation electronics and thus it is commonly used. An infrared system for broadcasting sensor readings in an Ariane VEB is studied in [2]. A real-time wireless sensor network is proposed in [4], taking the VEB environment into account and discussing the use of spatial diversity. Further work on infrared communications in this context — e.g., on bit error rates, diversity, and energy efficiency — can be found in [2], [3], [13], and [14].

Most related work is for applications with short payload packets and low data rates (e.g., for temperature, humidity, or pressure sensors). In contrast, our work employs a sensor network with data rates of several Mbps and payload sizes of 1023 bytes.

V. Conclusions

We implemented and deployed a testbed for high-speed UWB communication inside a space launch vehicle and evaluated the uplink from sensor nodes to APs using state-of-the-art commercial transceivers. The results show that the received power significantly varies over time but is still well above the sensitivity level for all studied node locations with a single AP. This offers an indication that UWB is a suitable technology in this environment, although further experimental studies are necessary to assess the reliability and quality of service demands of space applications.

Acknowledgments

This work was partly funded by the Carinthian Economic Promotion Fund (KWF) under grant 20214/26481/38805.

References

[1] D. Neuhold, J. Schmidt, J. Klaue, D. Schupke, and C. Bettstetter, "Experimental study of packet loss in a UWB sensor network for aircraft," in *Proc. ACM Int. Conf. on Modeling, Analysis and Simulation of Wireless and Mobile Systems (MSWiM)*, pp. 137–142, 2017.

[2] H. Kesuma, A. Ahmed, S. Paul, and J. Sebald, "Bit-error-rate measurement of infrared physical channel using reflection via multi layer insulation inside in ARIANE 5 vehicle equipment bay for wireless sensor network communication," in *Proc. IEEE Int. Conf. Wireless for Space and Extreme Environments (WiSEE)*, 2015.

[3] H. Kesuma, J. Sebald, and S. Paul, "Infrared wireless sensor network development for the Ariane launcher," in *Wireless Sensor Systems for Extreme Environments: Space, Underwater, Underground and Industrial*, pp. 151–168, Wiley, 2017.

[4] D. Tati, J. Klaue, and J. Sebald, "Reliable real-time wireless sensor networks using spatial diversity," in *Proc. IEEE Int. Conf. Wireless for Space and Extreme Environments (WiSEE)*, 2016.

[5] "DecaWave DW1000 User Manual." https://www.decawave.com/content/dw1000-user-manual, 2019-4-4.

[6] I. Schmidt, J. Jemai, R. Piesiewicz, R. Geise, M. Schwark, T. Kurner, M. Schirrmacher, and P. Thielker, "UWB propagation channels within an aircraft and an office building environment," in *Proc. IEEE Int. Symp. on Antennas and Propagation*, 2008.

[7] M. Jacob, K. L. Chee, I. Schmidt, J. Schuur, W. Fischer, M. Schirrmacher, and T. Kurner, "Influence of passengers on the UWB propagation channel within a large wide-bodied aircraft," in *Proc. European Conf. on Antennas and Propagation*, 2009.

[8] C. Spiliotopoulos and A. Kanatas, "Path-loss and time-dispersion parameters of UWB signals in a military airplane," *IEEE Antennas Wireless Propag. Lett.*, vol. 8, pp. 790–793, 2009.

[9] C. Sanchez, "Wireless sensor networks on-board aircrafts: Design and implementation of the medium access control protocol," Master's thesis, Universitat Politecnica de Catalunya, 2013.

[10] H. Saghir, C. Nerguizian, J. Laurin, and F. Moupfouma, "In-cabin wideband channel characterization for WAIC systems," *IEEE Trans. on Aerospace and Electronic Syst.*, vol. 50, no. 1, pp. 516–529, 2014.

[11] H. Bai, M. Atiquzzaman, and D. Lilja, "Wireless sensor network for aircraft health monitoring," in *Proc. IEEE Int. Conf. Broadband Networks*, 2004.

[12] R. K. Yedavalli and R. K. Belapurkar, "Application of wireless sensor networks to aircraft control and health management systems," *J. Control Theory Appl.*, vol. 9, no. 1, pp. 28–33, 2011.

[13] H. Kesuma, S. Schmale, S. Paul, and J. Sebald, "Low power asic design for infrared sensor network inside ARIANE 5 vehicle equipment bay," in *Proc. IEEE Int. Conf. Wireless for Space and Extreme Environments (WiSEE)*, 2016.

[14] H. Kesuma, T. Ahobala, S. Paul, and J. Sebald, "Ariane 5 space launcher vehicle equipment bay wireless sensor network telemetry subsystem with smart sensors," in *Proc. Europ. Telemetry and Test Conf. (ETTC)*, 2016.